



1 **Context-dependent plant–soil regulation of tree water transport in tropical forests**

2

3 Mahmuda Islam[†], Md. Morsalin[†], Md. Shakirul Islam Shavi, Saima Hossain Charu, Fahmida

4 Sultana, Mohammed Abu Sayeed Arfin-Khan, Mizanur Rahman*

5

6 *Department of Forestry and Environmental Science, Shahjalal University of Science and
7 Technology, Sylhet 3114, Bangladesh*

8

9 [†] These authors contributed equally to this work.

10 * Corresponding author, email: mizan-for@sust.edu

11

12 **Abstract**

13

14 Plant water transport is a key process linking vegetation physiology with soil and atmospheric
15 conditions and regulating ecosystem water and carbon fluxes. Yet, how intraspecific hydraulic
16 strategies vary across heterogeneous tropical environments remains poorly constrained. We
17 investigated hydraulic architecture of *Mangifera sylvatica*, a canopy tree species of South
18 Asian moist tropical forests, across two climatically and edaphically contrasting sites in
19 Bangladesh. Stem and branch xylem anatomical traits were quantified to estimate theoretical
20 hydraulic conductivity and percent loss of conductivity, alongside measurements of tree
21 structural attributes and soil physical and chemical properties. Despite pronounced differences
22 in elevation, soil texture, moisture availability, and stand structure between sites, hydraulic
23 strategies—including conductivity, vessel traits, and safety–efficiency trade-offs—were
24 conserved across forests. In contrast, the mechanisms regulating hydraulic function differed
25 strongly between sites, with crown architecture and soil sand content dominating in the drier
26 site, and sapwood allocation, tree height, and soil bulk density governing hydraulic behavior
27 in the wetter site. These results indicate that similar hydraulic outcomes can emerge from
28 distinct plant–soil–atmosphere interactions across space. Such context-dependent regulation of
29 plant water transport has implications for predicting tropical forest transpiration, drought
30 sensitivity, and land–atmosphere feedbacks under increasing vapor pressure deficit and climate
31 change.

32

33

34



35 **Short summary**

36 This study investigates how plant–soil interactions regulate tree water transport across
37 contrasting tropical forests in South Asia. Using xylem anatomical traits, hydraulic
38 conductivity estimates, and soil and structural measurements, we show that a tropical canopy
39 tree maintains conserved hydraulic strategies across environments but through different plant–
40 soil regulatory mechanisms. These findings provide process-based insight into vegetation
41 water transport and its role in ecosystem water fluxes under changing climate.

42

43 **Key words:** Xylem hydraulic traits, Safety–efficiency trade-off, Tropical moist forests,
44 *Mangifera sylvatica*, Hydraulic conductivity, Trait–environment relationships, Climate
45 vulnerability

46

47 **1. Introduction**

48 Water is required to perform tree's biological function, including maintaining stomatal
49 conductance and CO₂ uptake during photosynthesis (Gleason et al., 2016). Understanding trees
50 water conducting system is crucial for predicting their survival and function. Xylem vessels in
51 trees conduct water from the soil to the leaves (Sperry et al., 2008) and thus xylem hydraulic
52 traits are critical determinants of plant performance and survival particularly when trees
53 experience higher atmospheric demand under climate change (Choat et al., 2018). These
54 hydraulic traits not only indicate species-level drought tolerance but also represent how trees
55 adapt to fluctuations in climate-driven variables such as temperature, soil moisture, and vapor
56 pressure deficit (VPD)(Anderegg et al., 2016; Brodribb et al., 2020).

57 As global temperatures rise, the atmospheric vapor pressure deficit (VPD) also
58 increases, which causes water stress and higher rates of tree mortality risks (McDowell et al.,
59 2022). Tropical forests are amongst the vulnerable forest ecosystems to climate change
60 (Rahman et al., 2017; Wright, 2005) . The rise in global temperatures and the corresponding
61 increase in atmospheric VPD can significantly raise the risk of hydraulic failure in tropical tree
62 species (Grossiord et al., 2020). For example, recent studies projected that rising VPD could
63 reduce tropical forest productivity by up to 50% by 2100 (Staal et al., 2020). As VPD increases,
64 plants are forced to balance hydraulic efficiency with safety (Gleason et al., 2016), often
65 resulting in trade-offs in wood anatomy that influence both their growth and survival (Olson et
66 al., 2021).

67 To cope with climate-driven stressors, tropical trees exhibit diverse hydraulic strategies
68 involving structural, anatomical, and functional adaptations (Chowdhury et al., 2023; Islam et



69 al., 2025) . Structural attributes (e.g., tree height, DBH, crown traits etc.) modulate water use
70 efficiency at the stand level (Olson et al., 2021; Rahman et al., 2020). Wood anatomical
71 adaptations, including adjustments in vessel diameter, vessel density, sapwood specific
72 hydraulic conductivity directly influence the safety-efficiency tradeoff (Ferdous et al., 2023;
73 Gleason et al., 2016). Complementary functional traits (e.g., wood density, bark thickness) also
74 regulate hydraulic resilience (Anderegg et al., 2018). However, variation in site-level factors
75 (e.g., elevation, disturbance, slope, soil texture, pH, porosity, bulk density, organic matter, and
76 moisture etc.) might result in diverse hydraulic strategies even within the same species. For
77 instance, contrasting environments may affect how wood reacts anatomically in different ways,
78 which in turn affects the vulnerability or resistance to hydraulic failure (Pfautsch et al., 2016;
79 Schultdt, B., Knutzen, F., Delzon, S., Jansen, S., Müller-Haibold, H., Burlett, R., 2016). Yet, it
80 is still unknown whether species use the same hydraulic strategies in different population
81 structures and growing conditions, especially in tropical biomes that aren't well studied,
82 particularly in South Asian moist tropical forests.

83 Despite their ecological significance, South Asian moist tropical forests remain
84 understudied in terms of tree hydraulic functioning. There is a lack of research that combines
85 population-level traits, environmental variation, and wood anatomy, which limits our
86 understanding of species resilience in this region (Rahman, Islam, & Bräuning, 2019). This gap
87 is crucial, given that South Asian moist tropical forests particularly those in Bangladesh are
88 increasingly threatened by climate stressors such as more intense monsoons and rising
89 temperatures (Jihan et al., 2025).

90 *M. sylvatica*, a canopy tree endemic to these forests, serves as an ideal model to
91 investigate hydraulic responses because of its wide distribution across diverse landscapes. In
92 this study, we examine the xylem hydraulic strategies of *M. sylvatica*, a native tropical tree
93 species, across two moist forest sites in Bangladesh that have different population structures
94 and site characteristics. Specifically, we address two research questions:

95 (i) Does variation in population structure and site conditions lead to different hydraulic
96 strategies in naturally growing *M. sylvatica* across moist forests?

97 (ii) Which factors do regulate hydraulic behavior across moist forests with contrasting
98 population structure and growing conditions.

99

100 **2. Materials and methods**

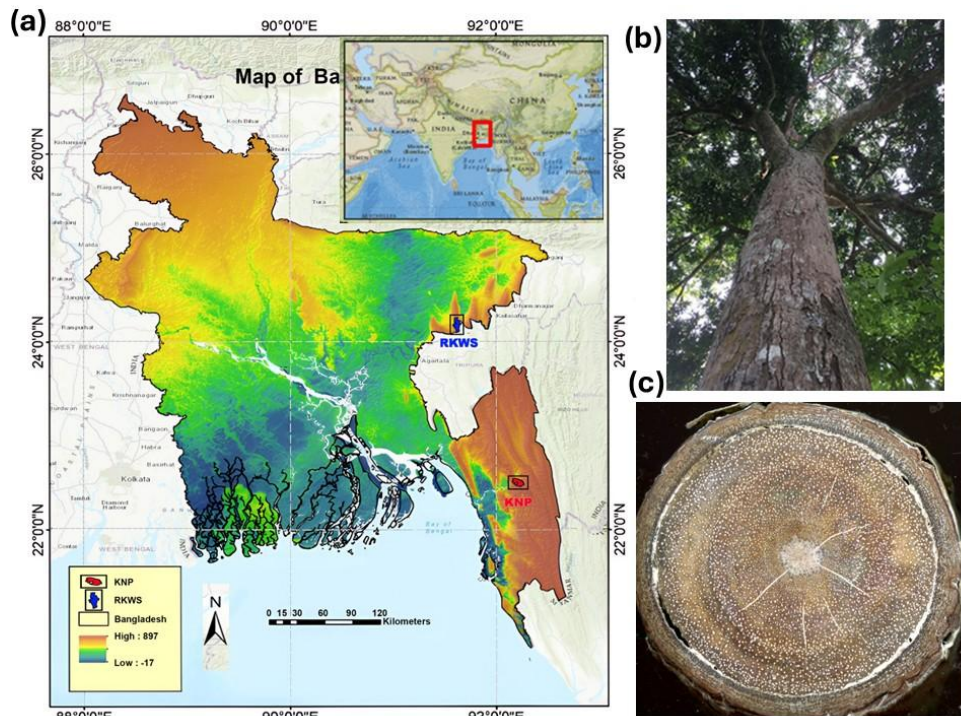
101 **2.1 Study sites, species, and sampling design**



102 This research was carried out in two distinct hill forests of Bangladesh: Rema-Kalenga
103 Wildlife Sanctuary (RKWS) and Kaptai National Park (KNP). RKWS lies between 24°06' -
104 24°14' N and 91°34'-91°41' E with an area of 1,795 hectares, encompassing the Southeastern
105 part of Tarap Hill Reserve of Northeastern Bangladesh. RKWS represents a moist tropical
106 climate with a mean annual temperature of 24.8 °C (highest in August about 33.3 °C and lowest
107 in November about 10.1 °C. The mean annual rainfall is 2363 mm averaged over 1950 to 2020.
108 The monthly average humidity varies from 74% to 89%. The study area consists of hills with
109 a maximum elevation of 100m (a.s.l.) as well as the flood plain valleys. Soil on the hills are
110 sandy loamy, whereas those on the low-lying area are clay loamy. It is tropical evergreen to
111 semi-evergreen hill forest. The sanctuary has a high conservation value due to its unique flora
112 and fauna. Some major tree species are *Dipterocarpus turbinatus*, *Schima wallichii*, *Tectona*
113 *grandis*, *Chukrasia tabularis*, *Toona ciliata*, *Hopea scaphula*, *Albizia procera*, *Syzygium*
114 *grandis*, and *Gmelina arborea*.

115 KNP is located between 22°29.991' N and 92°10.722' E in the hill tracts of Southeastern
116 part of Bangladesh. It encompasses with 5,465 hectares areas zzyyzz. The region has a tropical
117 monsoon climate, with average maximum temperature is 34°C and average minimum
118 temperature is 18°C. The mean annual rainfall is 2589 mm. This nature reserve consists of
119 tropical ever-green to semi-evergreen forests interspersed with hills, hillocks, and plainlands.
120 Some major species are *Chukrasia tabularis*, *Artocarpus heterophyllus*, *Artocarpus chama*,
121 *Acacia catechu*, *Acacia mangium*, *Acacia nilotica*, *Albizia procera*, *Toona ciliata*, *Erythrina*
122 *variegate*, *Dipterocarpus turbinatus*, *Syzygium grande*.

123



124

125

126 Figure 1. a) Map of Bangladesh showing the study sites: Rema-Kalenga Wildlife Sanctuary
127 (RKWS), and Kaptai National Park (KNP). b) A mature *Mangifera sylvatica* tree. c) a scanned
128 image of the cross-sectional surface of a *M. sylvatica* branch.

129

130 We selected *M. sylvatica* as a model tree mainly because this is one of the major native
131 canopy tree species in both study sites and has conservation values since the species has
132 recently been enlisted in the IUCN red list of threatened species (Akhter et al., 2022; Khan et
133 al., 2001). *M. sylvatica* is an evergreen light-demanding tree (Baul et al., 2016), forms annual
134 growth ring boundary (Islam et al., 2018a) and is suitable for wood anatomical measurements.

135 We established a total of 60 circular plots of 400 m² (plot radius 11.3 m) centering an
136 individual of *M. sylvatica* tree in two study sites (RKWS and KNP). Since *M. sylvatica* trees
137 naturally occurred, their distribution is sporadic and therefore a purposive sampling strategy
138 was followed to locate the position of *M. sylvatica* tree and to establish circular plots.
139 Biogeographic and tree demographic data, soil samples, wood samples of both branch and
140 stems, and leaf samples were collected from each plot. Soil samples were collected using a
141 soil auger at 15 cm depth. A total of five soil samples were taken from each plot following the



142 sampling criteria described by (Islam et al., 2016). The five soil samples were mixed and made
143 a composite soil sample that was analyzed for soil texture and soil moisture content
144 measurement. Soil samples collected using a soil core were analyzed for soil bulk density and
145 soil organic carbon measurement. A list of variables studied is shown in Table 1.

146

147 Table 1. List of biogeographic variables, tree structural attributes and hydraulic traits studied
148 in the present study conducted across two moist forest sites in Bangladesh.

149

Category	Variables	Abbreviation and unit
Hydraulic traits	Percent loss in theoretical conductivity from stem to branch	PLC _{(theo.)%}
	Theoretical stem hydraulic conductivity	K _{s-stem} (Kgm ⁻¹ s ⁻¹ MPa ⁻¹)
	Hydraulically weighted vessel diameter	DH _{stem} (mm)
	Xylem vulnerability index	Vx
	Stem vessel density	VD _{stem} (mm ²)
	Stem mean vessel area	MVA _{stem}
	Soil bulk density	SBD (gcm ⁻³)
Soil variables	Soil Porosity	P (%)
	Soil moisture content	SM (%)
	Soil organic carbon content	SOC (%)
	Soil pH	pH
	Clay content	Clay (%)
	Silt content	Silt (%)
	Sand content	Sand (%)
Biogeographic variables	Elevation	Elevation (m)
	Slope	Slope (degree)
	Disturbance index	DI
	Light interception index	LI
Tree structural attributes	Tree diameter at breast height	DBH (cm)
	Tree height	Height (m)
	Bark thickness	BT (cm)
	Crown surface area	CSA (m)
	Sapwood length	SL (cm)
	Wood density	WD (gcm ⁻³)

150

151 2.2. Biogeographic and environmental data collection

152 Biogeographic information, and demographic and environmental data collection were
153 carried out in each plot. Tree diameter at breast height (DBH), tree height, and crown surface
154 area (CSA) were measured for each sampled tree. Tree DBH was measured using a metric
155 diameter tape and tree height was measured using a Suunto clinometer (Suunto PM5/360PC



156 Clinometer, Finland). Tree CSA is usually derived from crown radius assuming tree crown as
157 circular shape and thus tree CSA was calculated from the formula of the area of a circle as
158 follows (Pretzsch et al., 2015; Rahman et al., 2021):

159
$$CSA = \pi r^2, \text{ Where } r = \text{crown radius.}$$

160 Crown radius is the distance between the center of the trunk and the perimeter of the crown.
161 Crown radii were measured in four directions and averaged to get the mean crown radii
162 (Pretzsch et al., 2015). Similarly, basal area (BA) was calculated from the diameter at breast
163 height (DBH) using the formula of the area of a circle.

164 Sapwood length and bark thickness were measured immediately after the extraction of
165 increment cores in the field. Sapwood was identified by its light brown color from the dark
166 brown heartwood portion. We did these measurements in the field because the differences in
167 color between sapwood and heartwood become less visible when cores dry. In addition, the
168 attack by stain fungi may further complicate the sapwood and heart wood identification. We
169 assigned a disturbance index value (1-5) to each sampled tree where 1 = Very low disturbed, 2
170 = low disturbed, 3 = moderate disturbed, 4 = high disturbed, 5 = very high disturbed. We also
171 assigned a light Interception value (1-5) to each sampled tree following the established
172 protocol as follows: 1 = crown received neither overhead nor lateral light, 2 = crowns received
173 no overhead high but received intermediate lateral light, 3 = crowns received partial light (10–
174 90%) from the vertical direction, 4 = crowns were fully exposed to vertical light (greater than
175 90%), 5 = crowns were completely exposed to both vertical and lateral light (Clark and Clark,
176 1992).

177

178 **2.3. Wood sample collection, processing and surface preparation**

179 A total of 180 increment cores of *M. sylvatica* were extracted from two study sites. All
180 the wood cores were taken at breast height (1.3 m) using a 5.15 mm increment borer. After
181 extraction, the cores were placed in a plastic core holder immediately to prevent them from any
182 mechanical breakdown. The wood cores were air dried for 24 hours to avoid any fungal attack.
183 A total of 60 branch samples were also collected from the two study sites. Branch samples were
184 collected through a sharp wood cutter. After collecting, all the samples were labeled properly
185 and dried accordingly following the same procedure used for increment cores.

186 The cores were placed on wooden holders and sanded using fine grain papers starting
187 at 120 grit and going up to 2000 grit until the anatomical details of the wood were clearly
188 visible. The dust was cleared using an air blower after sanding with each sandpaper grade.
189 After sanding white chalk was applied on the sanding surface of the core to fill the vessels that



190 improves the visibility of the vessels (Islam et al., 2018b). Then, cores were scanned at 2000
191 dpi by using a flatbed scanner (Epson Perfection V550 scanner, Epson America, Inc. CA). The
192 branches were also sanded following the same methodology but here we used fine grain papers
193 starting at 60 grit due to the coarse anatomical structure of bark portion and going up to 2000
194 grit until the anatomical details of the wood were clearly visible. Branches were then scanned
195 at 2000 dpi.

196 The sapwood area was identified on the scanned image of each tree and wood
197 anatomical measurements were made on the sapwood areas using the WinCELL image analysis
198 software (Regent instrument Inc, Quebec Canada). In the sapwood area of each core, three
199 2mm*2mm analyzed areas were taken for the vessel measurement. Similar measurement
200 protocol was followed for the branch samples. In each branch, three (2mm*2mm) areas were
201 taken from the last five growth rings for the vessel measurement.

202

203 **2.4. Wood anatomical measurement and calculation of hydraulic traits**

204 Vessel density (VD) and hydraulically weighted vessel diameter (DH) were measured
205 to calculate theoretical hydraulic conductivity (KS) from both stem cores and branches. VD
206 was calculated by counting the number of vessels per unit analyzed area. The radial and
207 tangential diameter of vessels were measured using the WinCELL software. Then, the
208 following equation was used to calculate the Hagen-Poiseuille hydraulically weighted vessel
209 diameter:

$$210 \quad DH = \sqrt[4]{\frac{1}{n} \sum_{i=1}^n \frac{2a^2b^2}{a^2+b^2}}, \quad (\text{Tyree and Zimmermann, 2002})$$

211 Here, n = Total number of vessels measured, a = Radial axes of vessels (mm), and b=
212 Tangential axes of vessels (mm).

213 The theoretical hydraulic conductivity (Ks) was measured according to the following formula:
214 (Hagen-Poiseuille's law)

$$215 \quad Ks = \left(\frac{\pi \rho}{128 \eta} \right) * DH^4 * VD; \quad (\text{Fan et al., 2012; Tyree and Zimmermann, 2002})$$

216 Here, η = Viscosity of water (1.002×10^{-9} MPa s $^{-1}$), ρ = Density of water at 20 °C (998.21 kgm $^{-3}$)
217 Finally, the Percentage Loss in Hydraulic Conductivity (PLC $_{\text{theo.}}\%$) from stem to branch was
218 measured using the following formula:

$$219 \quad PLC_{\text{theo.}}\% = (Ks_{\text{stem}} - Ks_{\text{Branch}}) / Ks_{\text{stem}} \times 100 \quad (\text{Schönauer et al., 2023})$$

220 Here, $Ks_{(\text{stem})}$ = Stem hydraulic conductivity (Kgm $^{-1}$ s $^{-1}$ MPa $^{-1}$), $Ks_{(\text{Branch})}$ = Branch hydraulic
221 conductivity (Kgm $^{-1}$ s $^{-1}$ MPa $^{-1}$).



222

223 **2.5. Measurement of sapwood density**

224 For the measurement of wood density (WD), an increment core for each tree was oven
225 dried. First, sapwood portion from each core was carefully dissected. The length and diameter
226 of each sapwood sample was measured. Cores were dried using an electric oven for 72 hours
227 at 105° C. The volume of fresh sapwood sample was calculated using the formula of a cylinder
228 as follows:

229
$$\text{Sapwood volume, } V (\text{cm}^3) = \pi r^2 h,$$

230 Where, r = Radius of the fresh sapwood core sample (cm), h = length of the fresh sapwood
231 sample (cm).

232 The density of sapwood of each tree was calculated using the following formula:

233
$$\text{Density (gm/cm}^3) = \text{Dry mass of sapwood (gm) / Volume of fresh sapwood (cm}^3)$$

234

235 **2.6. Measurement of soil moisture content, bulk density, and porosity**

236 Soil moisture content was determined using the oven-dry method. Fresh soil samples
237 were weighed to obtain the moist weight (M), oven-dried at 105 °C for 24 h, cooled to
238 approximately 50 °C, and reweighed to determine the dry weight (D). Moisture content (MC)
239 was then calculated as:

240
$$\text{MC (\%)} = \frac{M - D}{D} \times 100$$

241 Soil bulk density (SBD) was measured using the core method as described by Cresswell and
242 Hamilton (2002). Soil samples were collected with a cylindrical core of known dimensions,
243 and the core volume (V) was calculated as:

244
$$V (\text{cm}^3) = 3.14 \times \text{core radius}^2 \times \text{core height}$$

245 The oven-dry soil weight was divided by the core volume to obtain soil bulk density:

246
$$\text{SBD (g cm}^{-3}) = \frac{\text{Dry Soil Weight (g)}}{\text{Soil Volume (cm}^3)}$$

247 Soil porosity, a key physical property influencing soil structure and health, was estimated
248 following Pagliai and Vignozzi (2006). Porosity (P) was calculated as:

249
$$P (\%) = \left(1 - \frac{\text{Bulk density}}{\text{Particle density}}\right) \times 100$$

250 where particle density (PD) was obtained as:

251
$$PD = \frac{\text{Mass of soil (g)}}{\text{Volume of soil particles (cm}^3)}$$

252 and the volume of soil particles was computed using:

253
$$\text{Volume} = \pi r^2 h$$



254 All soil samples were oven-dried at 105 °C for 24 h, and weights were measured using a balance
255 with a sensitivity of 0.01 g.

256

257 **2.7. Soil pH and organic carbon measurement**

258 Soil pH was measured using a digital pH meter (Hanna HI2211 pH/ORP meter). For
259 each sample, 5 g of moist soil was placed in a 50 mL test tube, and 10 mL of distilled water
260 was added. The suspension was stirred for 10–15 minutes using an electric shaker, and the pH
261 was recorded directly from the meter display.

262 Soil organic carbon (SOC) was determined following the Loss on Ignition (LOI)
263 method (Viscarra Rossel et al., 2014). Soil samples were first oven-dried at 105 °C for 24 h to
264 obtain dry weight. A subsample of 10 g of oven-dried soil was placed in pre-weighed crucibles
265 and combusted in a muffle furnace at 550 °C for 4 h. Crucibles were then cooled inside the
266 furnace, and the post-combustion weight was measured. SOC content was estimated as the
267 proportion of weight lost during combustion relative to the oven-dry mass.

268

269 **2.8. Measurement of soil texture**

270 Soil texture was determined using the hydrometer method (Bouyoucos, 1962), which
271 measures the relative proportions of sand, silt, and clay in soil suspensions. A calibrated
272 hydrometer (ASTM No. 152 H with Bouyoucos scale in g/L) was used to record suspension
273 density at specific time intervals. The corrected hydrometer reading (Rc) was calculated as:

$$274 \quad Rc = (R - RL) + (t - 20) \times 0.3$$

275 where R = hydrometer reading at time t , RL = blank reading in distilled water, and T =
276 suspension temperature (°C).

277 Particle size fractions were then calculated as:

$$278 \quad \text{Silt\%+Clay\%} = (Rc \text{ at 40 sec}/\text{Dry Weight of sample soil}) \times 100$$

$$279 \quad \text{Clay\%} = (Rc \text{ at 2 hrs}/\text{Dry Weight of sample soil}) \times 100$$

$$280 \quad \text{Silt\%} = (\text{Silt\%+Clay\%}) - \text{Clay\%}$$

$$281 \quad \text{Sand\%} = 100 - (\text{Silt\%+Clay\%})$$

282 For each analysis, 40 g of air-dried soil was dispersed in distilled water, pre-treated
283 with 5 mL of 30% hydrogen peroxide when organic matter content exceeded 5%. The
284 suspension was heated on a hot plate for 15 min, cooled, and treated with 100 mL of 5% sodium
285 hexametaphosphate ($\text{Na}(\text{PO}_3)_6$) as a dispersing agent. The solution was then transferred to a
286 1000 mL sedimentation cylinder, diluted to volume with distilled water, and stirred
287 mechanically for 3 min. Hydrometer readings were taken at 40 seconds and 2 hours after



288 mixing, with concurrent temperature measurements. Blank readings were obtained using the
289 dispersing solution alone.

290

291 **2.9. Data analysis**

292 The *readxl*, *dplyr*, *tidyverse* packages were used to organize and clean data.
293 Principal Component Analysis (PCA) was performed using *FactoMineR*, *factoextra*, *corr*,
294 *corrplot*, and *ggcorrplot* packages to explore the multivariate relationships between hydraulic
295 traits, tree demographics, and soil physical–chemical properties. The loading vectors indicate
296 the relative importance and correlation among variables, where vector length corresponds to
297 correlation strength and the angle between vectors reflects their relationships (acute = positive,
298 obtuse = negative, right angle = no correlation). Independent sample t-test was performed using
299 the *stats* package to compare the population structure and site conditions between two study
300 sites. Similar t-test was also performed to evaluate the differences in hydraulic traits between
301 stem and branch and between two sites. A simple linear regression was performed using *ggpubr*
302 package to test the relationship of hydraulic traits with tree structural attributes, functional
303 traits, and environmental variables. The difference in slope of the linear relationship between
304 two sites was evaluated employing analysis of covariance (ANCOVA) using *car* and *broom*
305 packages. To evaluate the relative importance of each significant variable in predicting
306 hydraulic strategies, we performed linear mixed effect modelling (LMEM) using the *nlme*
307 package, taking tree attributes and environmental variables as fixed factors and tree ID as
308 random factor. Standardized model coefficients and 95% confidence intervals were extracted
309 using *broom.mixed* package. We calculated both conditional and marginal R^2 and used Akaike
310 Information Criterion (AIC) using *MuMin* package to evaluate the model performance. All
311 analyses were performed in R using the version 4.5.1 (Great Square Root) (R Development
312 Core Team, 2025).

313

314 **3. Results**

315

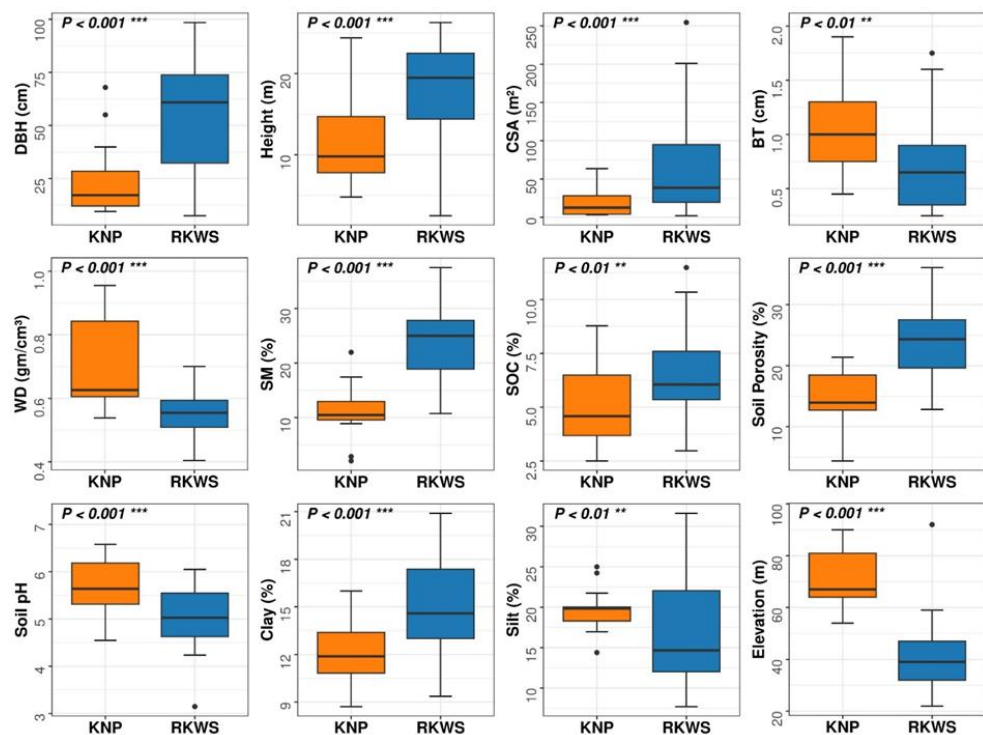
316 **3.1. Variation in population structure and growing conditions between sites**

317 The population of *M. sylvatica* in RKWS had significantly higher DBH, height and
318 CSA ($p < 0.001$) with lower BT and WD ($p < 0.01$) than the population in KNP (Fig. 2). KNP
319 had *M. sylvatica* population at higher elevation (mean elevation 71 m above sea level)
320 compared to RKWS (40 m) ($p < 0.001$). The population of *M. sylvatica* in RKWS was grown in
321 soils with higher SM ($p < 0.001$), higher SOC ($p < 0.01$), higher soil porosity ($p < 0.001$) and lower



322 pH ($p < 0.001$) than KNP. In terms of soil texture, RKWS supported *M. sylvatica* population in
323 soils with higher clay content ($p < 0.001$) and lower silt ($p < 0.01$) content than KNP (Fig. 2).
324 However, there was no significant difference in LI, DI, slope, sand content, SBD, SL, and WD
325 between the two sites inhabiting *M. sylvatica* population (Table S1).

326



327
328 Figure 2. Comparing population structure and growing conditions of *Mangifera sylvatica*
329 across two moist forest sites in Bangladesh.

330

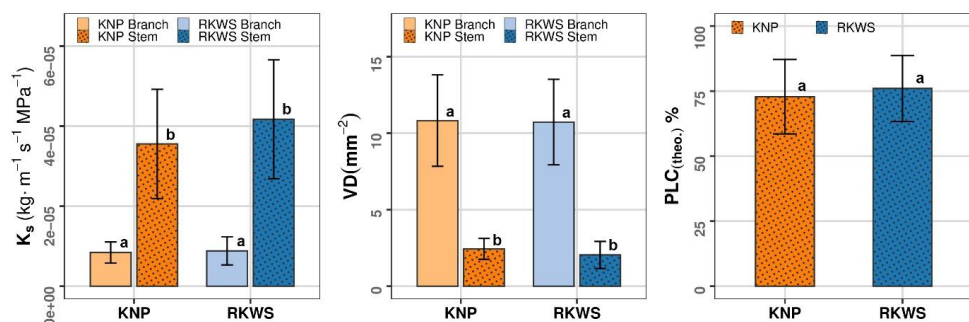
331 3.2. Hydraulic strategies of *M. sylvatica* across sites

332 The independent sample t-test revealed no significant difference in Ks, VD, and
333 PLC_(theo.)% of *M. sylvatica* population between two sites (Fig. 3). However, within a site, stem
334 Ks was significantly higher than branch in the *M. sylvatica* population of KNP ($t = -14.1$,
335 $p < 0.001$). Likewise, a significantly higher Ks was found in stem than in branch at RKWS
336 ($t = 16.7$, $p < 0.001$). In contrast, VD was higher in branch than in stem in both sites ($p < 0.001$)
337 (Fig. 3). At KNP, Ks decreased by **72.4%** from Stem to Branch which is slightly lower
338 than RKWS with a decrease of 76 %.



339 We observed a significant trade-off between stem DH and VD in both sites with slightly
 340 higher slope in RKWS ($R^2=0.63$, $p<0.001$) than in KNP ($R^2=0.49$, $p<0.001$) albeit the
 341 difference in slope of the linear relationship between two sites was not significant as revealed
 342 by the ANCOVA test (Table S2). This site level vessel diameter and density trade-off also
 343 existed when we analyzed data from two sites together ($R^2=0.61$, $p<0.001$) (Fig. 4). Thus the
 344 *M. sylvatica* populations from two sites followed the same hydraulic strategies though they
 345 experienced different growing conditions and had different population structures.

346

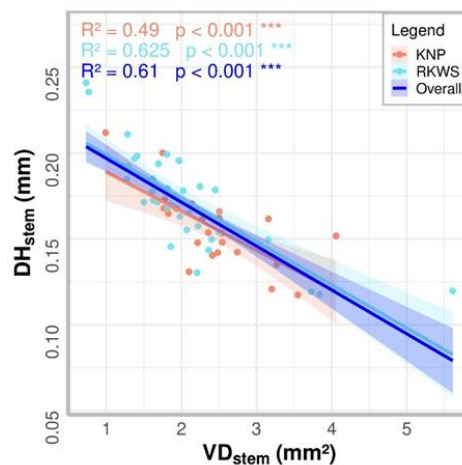


347

348

349 Figure 3. Comparison of stem and branch xylem hydraulic traits of *M. sylvatica* across two
 350 moist forest sites in Bangladesh.

351



352

353 Figure 4. Trade-off between hydraulically weighted vessel diameter, Dh (Hydraulic
 354 efficiency) and vessel density, VD (hydraulic safety) in *Mangifera sylvatica* at two moist
 355 forest sites in Bangladesh.

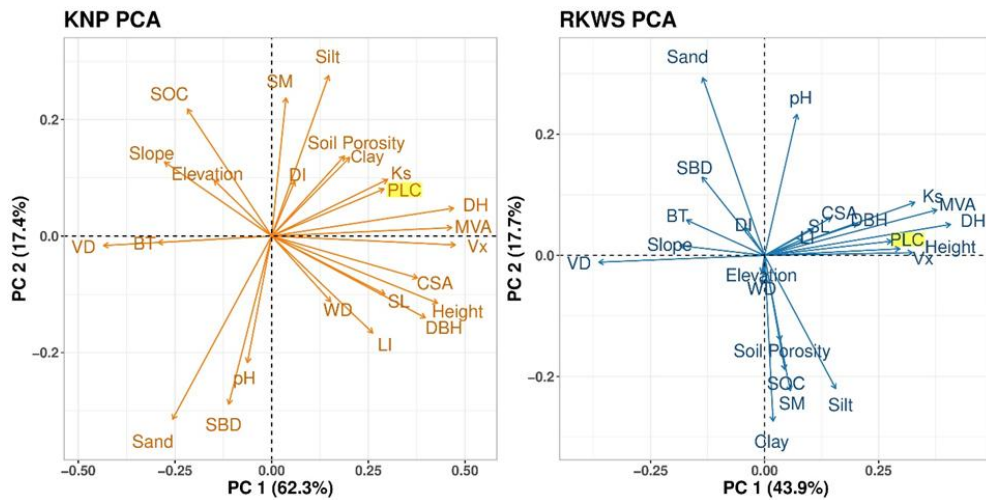


356

357 **3.3. Association between hydraulic traits, structural and functional attributes and site factors**

358 In KNP, the first two principal components explained nearly 80 % of the total variance
359 (PC1=62.3%, PC2=17.4%). PC1 was primarily influenced by DH, MVA, Vx, CSA, tree
360 Height, DBH, and SL. These vectors are closely aligned, indicating strong positive
361 interrelationships among these wood hydraulic traits and size metrics. In RKWS, PC1 and PC2
362 explained a total of 61.6% of the variance (PC1 = 43.9%, PC2 = 17.7%). Here, PC1 was most
363 strongly associated with CSA, DBH, Height, DH, MVA, and PLC_(theo.)%, indicating that in this
364 site, larger, wider vessels and bigger trees are strongly linked to greater conductivity loss (Fig
365 5).

366



367

368 Figure 5. Principal Component Analysis (PCA) results showing the association between site
369 factors, hydraulic traits, structural and functional attributes of *Mangifera sylvatica* across two
370 moist forest sites in Bangladesh. For variable names please refer to Table 1.

371

372 **3.4. Driving factors of hydraulic behavior**

373 The Ks of *M. Sylvatica* population in KNP showed a significant positive relationship
374 with CSA ($R^2= 0.26$, $p<0.05$), and tree height ($R^2= 0.20$, $p<0.05$), and a negative significant
375 relationship with sand content in soil ($R^2= 0.174$, $p<0.05$) (Fig. 6) but no significant
376 relationship with SL ($R^2=0.005$, $p=0.76$) and other variables. In RKWS, Ks of *M. sylvatica*
377 population showed a significant positive relationship with tree Height ($R^2= 0.21$, $p<0.01$), CSA

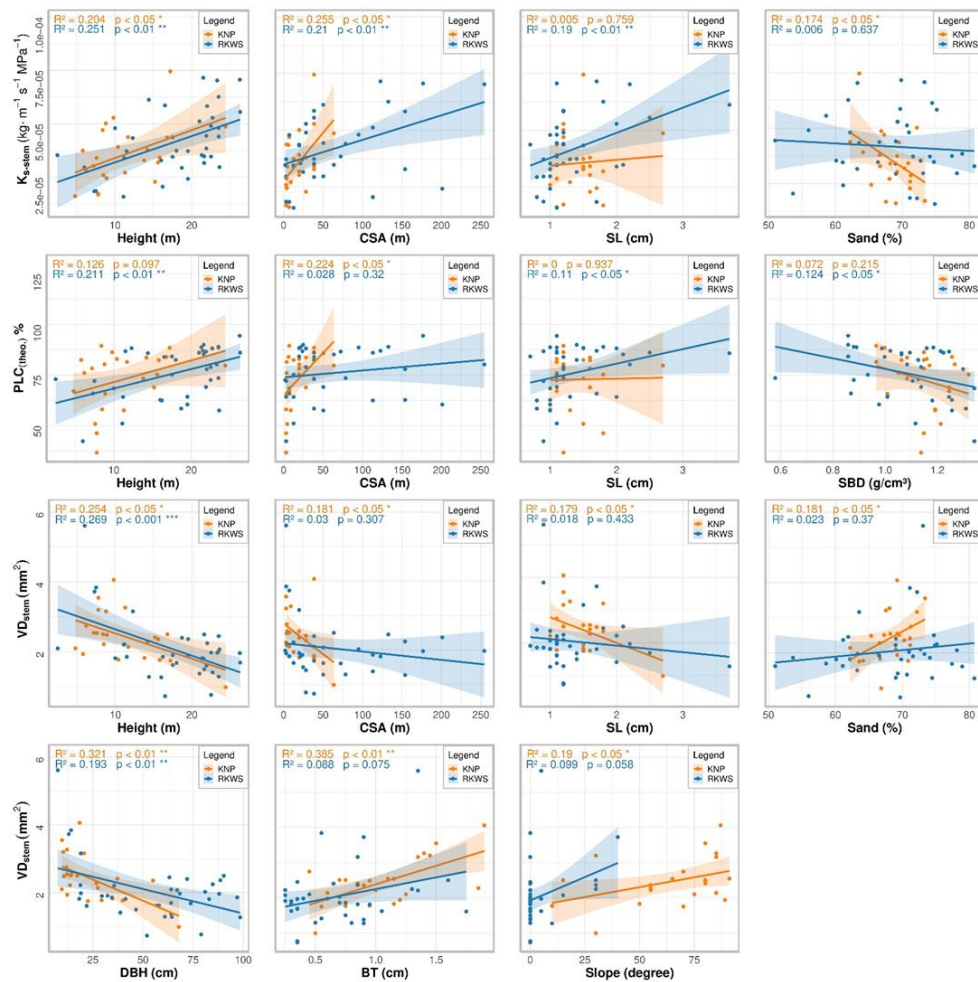


378 (R²=0.21, p<0.01), and SL (R²=0.19, p<0.01) but no significant relationship with soil sand
379 content (R²=0.006, p=0.64) and other variables.

380 The PLC_(theo.) of *M. Sylvatica* population in KNP showed a significant positive
381 relationship with CSA (R²= 0.22, p<0.05) but no significant relationship with tree height (R²=
382 0.13, p=0.10), SL (R²= 0.09, p=0.93), and SBD (R²= 0.07, p=0.21) and other variables. In
383 contrast, the PLC_(theo.) of *M. sylvatica* population in RKWS showed a significant positive
384 relation with tree height (R²= 0.21, p<0.01), SL (R²=11, p<0.05), and SBD (R²=0.12, p<0.05)
385 but but no significant relationships with CSA (R²= 0.03, p=0.32) and other variables.

386 The VD of *M. Sylvatica* population in KNP showed a significant negative relationship
387 with tree height (R²= 0.25, p<0.05), DBH (R²= 0.32, p<0.01), CSA (R²= 0.18, p<0.05), SL
388 (R²= 0.18, p<0.05) and significant postive relationship with slope (R²= 0.19, p<0.05), soil sand
389 content (R²= 0.181, p<0.05), and BT (R²= 0.385, p<0.01). In RKWS, the VD of *M. sylvatica*
390 population showed negative significant relationship with tree height (R²= 0.27, p<0.001), and
391 DBH (R²=0.19, p<0.01), but no significant relationship with any other variables (Fig 6).

392



393

394 Figure 6. Driving factors of hydraulic behavior in *Mangifera sylvatica* across two moist forest
 395 sites in Bangladesh.

396

397 Linear mixed effect modelling with significantly correlated variables as fixed factors
 398 and tree species identity as the random factors revealed the relative importance of each factor
 399 in predicting K_s , PLC(theo.), and VD in KNP and RKWS. The outputs of mixed effect models
 400 are shown in Table 2.

401

402 Table 2. Linear mixed effect modeling results for predicting K_s , VD, and PLC (theo.) in two
 403 moist forest sites in Bangladesh.

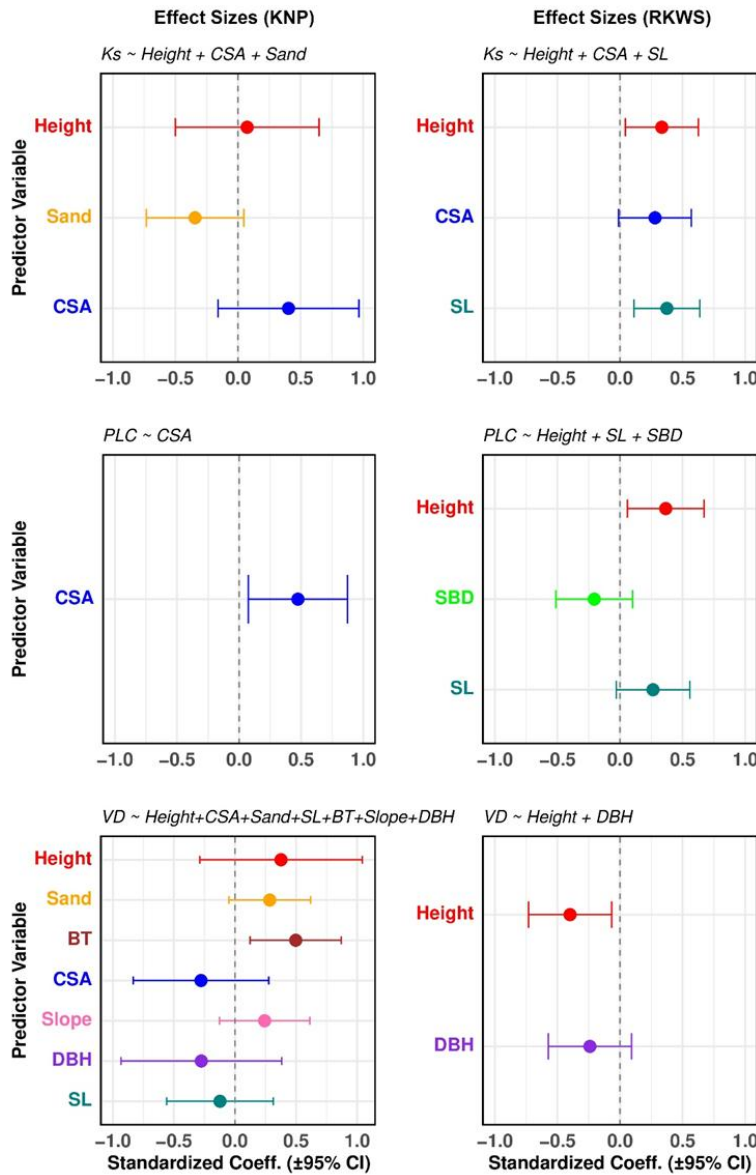
Response Variable	Study Site	Fixed Factors	AIC	Marginal R^2	Conditional R^2	P-values
-------------------	------------	---------------	-----	----------------	-------------------	----------



K _s	KNP	Height + CSA + Sand	-343.7282	0.3458081	0.9193462	<.0001
	RKWS	Height + CSA + SL	-620.4492	0.4367171	0.9305542	<.0001
PLC _(theo.)	KNP	CSA	186.8223	0.2160646	0.9033504	0.0225
	RKWS	Height + SL + SBD	276.3645	0.3086773	0.9147684	<.0001
VD	KNP	Height + CSA + Sand + SL + BT + Slope + DBH	80.27306	0.582859	0.9485717	0.1112
	RKWS	Height + DBH	107.9036	0.3010927	0.9138333	0.5895

404

405 Our mixed effect models revealed that CSA was the most important variable in
406 predicting K_s and PLC_(theo.) of *M. Sylvatica* population in KNP (Fig 7). The dominant factors
407 that drove VD of *M. Sylvatica* population in KNP were mostly the structural attributes of trees
408 including tree height, DBH, CSA, and BT. However, the highest contribution in explaining VD
409 variation in *M. Sylvatica* population in KNP was made by tree height and bark thickness as
410 indicated by the higher standardized coefficient (effect size) (Fig. 7). In RKWS, tree height,
411 DBH, and SL played significant rule in regulating K_s of *M. sylvatica* population with highest
412 contribution by SL followed by tree height and CSA (Fig. 7). Tree height also played the most
413 important role in determining PLC_(theo.) of *M. Sylvatica* population in RKWS. The VD variation
414 in *M. Sylvatica* population in RKWS was explained by tree two most important tree structural
415 attributes: tree height and DBH, with tree height as the most dominating factor (Fig. 7).



416

417 **Figure 7.** Standardized effect size derived from linear mixed-effect models for predicting
 418 site-specific hydraulic behavior across moist tropical forests in Bangladesh.

419

420 **4. Discussion**

421

422 **4.1. Population structure and environmental variation shaping local contexts**



423 Our study revealed pronounced differences in population structure and growing
424 conditions of *Mangifera sylvatica* across RKWS and KNP. Trees in RKWS were notably
425 larger—with higher DBH, greater height, and larger crown surface area—than those in KNP,
426 and grew in soils with higher moisture, greater porosity, higher organic carbon, and more clay.
427 Such structural divergence is typical of tropical forests where topography, soil formation,
428 disturbance history, and microclimate combine to generate steep ecological gradients over
429 relatively small spatial scales (Feroz et al., 2014; Islam et al., 2016). These factors influence
430 resource availability, below-ground water storage, rooting depth, and nutrient cycling, all of
431 which directly or indirectly affect hydraulic architecture.

432 The contrasting soil textures between sites are particularly noteworthy. Clay-rich soils
433 in RKWS likely retain moisture for longer periods and exhibit greater water-holding capacity
434 but may impose higher mechanical resistance to root penetration. In contrast, the sandier soils
435 of KNP drain rapidly and often create drier rooting zones, especially during dry seasons. Soil
436 moisture and textural variability are known to influence xylem anatomy by modulating water
437 availability and tension gradients within the hydraulic pathway (Pfautsch et al., 2016). Yet,
438 despite these strong environmental contrasts, *M. sylvatica* maintained statistically similar
439 hydraulic traits across sites—a striking indication of hydraulic trait stability.

440 The absence of site-level differences in wood density, sapwood length, and many other
441 functional traits further suggests that *M. sylvatica* possesses a conserved structural strategy that
442 may reflect evolutionary stability in its hydraulic architecture. Many tropical species exhibit
443 such trait conservatism, particularly those occupying relatively stable climatic ranges (Gleason
444 et al. 2016). However, the divergence in tree size, soil characteristics, and microclimate
445 between sites indicates that populations of the same species can experience significantly
446 different hydraulic challenges, making it crucial to understand how conserved hydraulic
447 strategies are maintained across such varied environments.

448

449 **4.2. Hydraulic strategies remain conserved despite ecological contrasts**

450 Across both sites, we observed remarkably similar hydraulic strategies, as evidenced
451 by comparable values of hydraulic conductivity (Ks), vessel density (VD), and theoretical
452 percent loss of conductivity (PLC). This finding strongly supports our hypothesis that *M.*
453 *sylvatica* maintains a consistent safety–efficiency balance regardless of local environmental
454 variations. Such conservatism is widely documented in tropical species and often emerges from



455 evolutionary constraints on xylem anatomy, which limits the extent to which hydraulic traits
456 can shift in response to local conditions (Brodribb et al., 2020; Gleason et al., 2016).

457 The universal decline in hydraulic efficiency from stem to branch (72–76%) across both
458 RKWS and KNP reflects a consistent within-tree hydraulic hierarchy. Branches exhibited
459 higher vessel density and smaller vessel diameters—suggests that increase hydraulic safety,
460 reduce cavitation risk, and ensure maintenance of water supply to leaves under fluctuating
461 atmospheric demand (Olson et al., 2021). Similar patterns have been widely observed in
462 tropical and temperate trees where distal organs act as hydraulic bottlenecks to enhance safety
463 margins (Sperry et al., 2008; Trifilo et al., 2014).

464 The strong trade-off between vessel diameter and vessel density in both sites provides
465 further evidence of this consistency. A larger D_h is associated with higher hydraulic efficiency
466 but increased vulnerability to embolism. Conversely, higher vessel density enhances safety by
467 making sure that some vessels remain functional while some vessels become blocked by
468 cavitation or embolism (Venturas, M.D., Sperry, J.S., Hacke, 2017). The slope and strength of
469 this trade-off were nearly identical between RKWS and KNP indicating that *M. sylvatica*
470 follows a fixed architectural strategy to balance risk and performance, likely reflecting
471 constraints imposed by its phylogeny and ecological niche (Fan et al., 2012).

472 The absence of site-level variation in hydraulic trait suggests that environmental
473 differences did not induce anatomical divergence. This pattern could arise from (i) stabilizing
474 selection maintaining optimal xylem design, (ii) developmental canalization limiting the
475 plasticity of xylem traits, or (iii) species-level adaptation to broad climatic envelopes rather
476 than local microhabitats. Together, these results provide strong evidence that *M. sylvatica* is
477 hydraulically conservative across the diverse moist forests in Bangladesh.

478

479 **4.3. Divergent trait–environment associations reveal site-specific mechanisms**

480 Although hydraulic traits remained consistent across sites, the multivariate patterns
481 revealed by PCA and regression suggest that different structural and environmental variables
482 regulate hydraulic function at each site. This finding reflects an important ecological nuance:
483 the strategy is uniform, but the pathways that sustain the strategy differ according to local
484 contexts.

485 In KNP, hydraulic efficiency aligned strongly with structural variables such as crown
486 surface area, DBH, tree height, and sapwood length. These results imply that in a drier, sandier
487 environment—where soil moisture is more limited—tree architecture plays a crucial role in



488 determining hydraulic performance. Larger crowns and taller stems demand greater water
489 transport capacity, explaining the strong association of K_s and D_h with crown traits. Similar
490 patterns have been documented in moisture-limited tropical forests where canopy architecture
491 influences water balance more than soil traits (Anderegg et al., 2018; Grossiord et al., 2020).
492 By contrast, in RKWS, hydraulic traits aligned most closely with tree height, sapwood length,
493 and soil bulk density. Clay-rich soils with higher porosity may create mesic but mechanically
494 challenging rooting environments, where sapwood allocation becomes more critical for
495 ensuring efficient water transport. Sapwood depth is known to buffer against water stress and
496 contributes significantly to the total conductive area (Chave et al., 2009; Meinzer et al., 2003).
497 The strong influence of sapwood length on hydraulic traits in RKWS therefore reflects the
498 increased role of internal water storage and radial conductivity in wetter, denser soils.

499 Moreover, PLC in RKWS was associated with soil bulk density and tree height,
500 whereas in KNP it was primarily linked to crown surface area. These divergent patterns reflect
501 how site-specific constraints—soil structure versus evaporative demand—shape conductivity
502 loss along the flow path. Together, these findings highlight that although hydraulic architecture
503 is conserved, *M. sylvatica* fine-tunes its structural and environmental relationships differently
504 at each site, demonstrating functional plasticity in the drivers but not in the outcome.

505

506 **4.4. Drivers of hydraulic behaviour vary across sites**

507 Mixed-effect modelling provided clearer insight into the relative contributions of
508 different drivers. In KNP, crown surface area was the dominant predictor of both K_s and PLC,
509 emphasizing the strong influence of canopy architecture in environments characterized by
510 higher evaporative demand and coarser soil texture. This suggests that trees in KNP adjust
511 water transport capacity to match transpirational demand imposed by crown size—a pattern
512 typical of trees in moisture-limited or seasonally dry conditions.

513 Conversely, in RKWS, sapwood length and tree height were the strongest drivers of K_s
514 and PLC, reflecting that water transport capacity in this wetter, clay-rich environment may be
515 more related to internal xylem allocation than canopy-driven demand. The importance of
516 sapwood variables in RKWS also suggests that trees in wetter sites rely on structural
517 redundancy and internal buffering to regulate hydraulic efficiency, which aligns with previous
518 studies showing that sapwood allocation increases in mesic environments where mechanical
519 resistance is higher (Schuldt, B., Knutzen, F., Delzon, S., Jansen, S., Müller-Haubold, H.,
520 Burlett, R., 2016). Vessel density exhibited strong associations with structural and



521 environmental factors in KNP but was primarily regulated by tree height and DBH in RKWS.
522 This again suggests that hydraulic safety is shaped more by environmental stressors in KNP
523 but by ontogenetic scaling in RKWS.

524 The divergence in drivers across sites suggests that *M. sylvatica* uses different
525 functional mechanisms to maintain a stable hydraulic balance in different environments. This
526 flexibility in trait–environment relationships may underpin the species’ ability to persist across
527 diverse South Asian moist forest ecosystems.

528

529 **4.5. Ecological and conservation implications under climate change**

530 The resilience of *M. sylvatica* under future climate conditions will depend on the
531 interaction between its conserved hydraulic architecture and its flexibility in structural and
532 functional drivers. Rising temperatures and increased atmospheric VPD are expected to
533 intensify hydraulic stress, particularly in tropical forests already near their physiological
534 thresholds (Choat et al. 2018; McDowell et al. 2022). Populations in KNP—where hydraulic
535 function relies heavily on crown traits and is sensitive to soil sand content—may become
536 especially vulnerable under scenarios of declining soil moisture. In contrast, RKWS
537 populations may be more buffered by sapwood allocation but could face limitations if rising
538 VPD exceeds the compensatory capacity of internal hydraulic storage.

539 Because *M. sylvatica* is listed as a threatened species, identifying populations most
540 vulnerable to water stress will be crucial for conservation planning. Our results suggest that
541 management strategies should be site specific: protecting soil moisture and reducing
542 disturbances in KNP, and maintaining stand structure and soil integrity in RKWS. The stability
543 of hydraulic traits across contrasting environments is encouraging, as it suggests a degree of
544 resilience to climatic variability. However, the limited plasticity in core hydraulic architecture
545 implies that the species’ adaptive capacity may rely more on structural adjustments (crown
546 architecture, sapwood depth) than on modifications to xylem anatomy.

547

548 **Conflict of interest statement**

549

550 The authors declare no conflicts of interest.

551

552 **Data availability statement**

553 All data supporting the manuscript can be found in the supplementary materials.



554

555 **Author contributions**

556

557 MI, MM, and MR conceptualized the study; MI, MR, MASA, FS, MM planned the field
558 campaign; MM, MSIS, SHC performed the measurements and laboratory analysis; MI, MR,
559 MM analyzed the data; MI and FS acquired funding; MR, MASA performed the validation of
560 analysis and results; MI MM wrote the first manuscript draft with important contribution from
561 MR; All authors contributed to the revision and editing of the manuscript.

562

563 **Acknowledgements**

564

565 We sincerely acknowledge the financial support from the Forest Department of Bangladesh
566 (BFD) under the project “Sustainable Forest and Livelihood, SUFAL” project. (Grant no.
567 FD/SUFAL/SIG (2nd call)/1160). We thank the research permits and logistical support by
568 BFD during fieldwork.

569

570 **References**

571

- 572 Akhter, S., McDonald, M., Jashimuddin, M., Bashirul-Al-Mamun, M., and Sarker, P.:
573 Agroforestry potential of a wild mango species (*Mangifera sylvatica* Roxb.), *Trees, For.*
574 *People*, 7, 100194, <https://doi.org/https://doi.org/10.1016/j.tfp.2022.100194>, 2022.
- 575 Anderegg, W. R. L., Klein, T., Bartlett, M., Sack, L., Pellegrini, A. F. A., Choat, B., and
576 Jansen, S.: Meta-analysis reveals that hydraulic traits explain cross-species patterns of
577 drought-induced tree mortality across the globe, *Proc. Natl. Acad. Sci.*, 113, 5024–5029,
578 <https://doi.org/10.1073/pnas.1525678113>, 2016.
- 579 Anderegg, W. R. L., Konings, A. G., Trugman, A. T., Yu, K., Bowling, D. R., Gabbitas, R.,
580 Karp, D. S., Pacala, S., Sperry, J. S., Sulman, B. N., and Zenes, N.: Hydraulic diversity of
581 forests regulates ecosystem resilience during drought, *Nature*, 561, 538–541,
582 <https://doi.org/10.1038/s41586-018-0539-7>, 2018.
- 583 Baul, T. K., Jahedul Alam, M., and Nath, T. K.: *Mangifera sylvatica* Roxb. in the Forests of
584 South-Eastern Bangladesh: A Potential Underutilised Tree for Small-Scale Forestry, *Small-
585 scale For.*, 15, 149–158, <https://doi.org/10.1007/s11842-015-9314-x>, 2016.
- 586 Bouyoucos, G. J.: Hydrometer Method Improved for Making Particle Size Analyses of Soils,
587 *Agron. J.*, 54, 464–465,



- 588 https://doi.org/https://doi.org/10.2134/agronj1962.00021962005400050028x, 1962.
- 589 Brodribb, T. J., Powers, J., Cochard, H., and Choat, B.: Hanging by a thread? Forests and
- 590 drought, *Science* (80-.), 368, 261–266, https://doi.org/10.1126/science.aat7631, 2020.
- 591 Chave, J., Coomes, D., Jansen, S., Lewis, S. L., Swenson, N. G., and Zanne, A. E.: Towards a
- 592 worldwide wood economics spectrum, *Ecol. Lett.*, 12, 351–366,
- 593 https://doi.org/10.1111/j.1461-0248.2009.01285.x, 2009.
- 594 Choat, B., Brodribb, T. J., Brodersen, C. R., Duursma, R. A., López, R., and Medlyn, B. E.:
- 595 Triggers of tree mortality under drought, *Nature*, 558, 531–539,
- 596 https://doi.org/10.1038/s41586-018-0240-x, 2018.
- 597 Chowdhury, T., Islam, M., and Rahman, M.: Long-term growth and xylem hydraulic
- 598 responses of *Albizia procera* (Roxb.) Benth. to climate in a moist tropical forest of
- 599 Bangladesh, *Perspect. Plant Ecol. Evol. Syst.*, 61, 125762,
- 600 https://doi.org/https://doi.org/10.1016/j.ppees.2023.125762, 2023.
- 601 Clark, D. A. and Clark, D. B.: Life History Diversity of Canopy and Emergent Trees in a
- 602 Neotropical Rain Forest, *Ecol. Monogr.*, 62, 315–344, https://doi.org/10.2307/2937114,
- 603 1992.
- 604 Fan, Z.-X., Zhang, S.-B., Hao, G.-Y., Ferry Slik, J. W., and Cao, K.-F.: Hydraulic
- 605 conductivity traits predict growth rates and adult stature of 40 Asian tropical tree species
- 606 better than wood density, *J. Ecol.*, 100, 732–741, https://doi.org/10.1111/j.1365-
- 607 2745.2011.01939.x, 2012.
- 608 Ferdous, J., Islam, M., and Rahman, M.: The role of tree size, wood anatomical and leaf
- 609 stomatal traits in shaping tree hydraulic efficiency and safety in a South Asian tropical moist
- 610 forest, *Glob. Ecol. Conserv.*, 43, e02453,
- 611 https://doi.org/https://doi.org/10.1016/j.gecco.2023.e02453, 2023.
- 612 Feroz, S. M., Alam, M. R., Das, P., and Al Mamun, A.: Community ecology and spatial
- 613 distribution of trees in a tropical wet evergreen forest in Kaptai national park in Chittagong
- 614 Hill Tracts, Bangladesh, *J. For. Res.*, 25, 311–318, https://doi.org/10.1007/s11676-013-0423-
- 615 0, 2014.
- 616 Gleason, S. M., Westoby, M., Jansen, S., Choat, B., Hacke, U. G., Pratt, R. B., Bhaskar, R.,
- 617 Brodribb, T. J., Bucci, S. J., Cao, K. F., Cochard, H., Delzon, S., Domec, J. C., Fan, Z. X.,
- 618 Feild, T. S., Jacobsen, A. L., Johnson, D. M., Lens, F., Maherli, H., Martínez-Vilalta, J.,
- 619 Mayr, S., Mcculloh, K. A., Mencuccini, M., Mitchell, P. J., Morris, H., Nardini, A.,
- 620 Pittermann, J., Plavcová, L., Schreiber, S. G., Sperry, J. S., Wright, I. J., and Zanne, A. E.:
- 621 Weak tradeoff between xylem safety and xylem-specific hydraulic efficiency across the



- 622 world's woody plant species, *New Phytol.*, 209, 123–136, <https://doi.org/10.1111/nph.13646>,
623 2016.
- 624 Grossiord, C., Buckley, T. N., Cernusak, L. A., Novick, K. A., Poulter, B., Siegwolf, R. T.
625 W., Sperry, J. S., and McDowell, N. G.: Plant responses to rising vapor pressure deficit, *New*
626 *Phytol.*, 226, 1550–1566, [https://doi.org/https://doi.org/10.1111/nph.16485](https://doi.org/10.1111/nph.16485), 2020.
- 627 Islam, M., Salim, S. H., Kawsar, M. H., and Rahman, M.: The effect of soil moisture content
628 and forest canopy openness on the regeneration of *Dipterocarpus turbinatus* C. F. Gaertn. (*629 Dipterocarpaceae*) in a protected forest area of Bangladesh, *Trop. Ecol.*, 57, 455–464, 2016.
- 630 Islam, M., Rahman, M., and Bräuning, A.: Growth-ring boundary anatomy and
631 dendrochronological potential in a moist tropical forest in Northeastern Bangladesh, *Tree- 632 Ring Res.*, 74, 76–93, <https://doi.org/10.3959/1536-1098-74.1.76>, 2018a.
- 633 Islam, M., Rahman, M., and Bräuning, A.: Long-Term Hydraulic Adjustment of Three
634 Tropical Moist Forest Tree Species to Changing Climate, *Front. Plant Sci.*, 9, 1761,
635 <https://doi.org/10.3389/fpls.2018.01761>, 2018b.
- 636 Islam, M., Afia, F. A., Borsa, A. Das, Tipu, M. T. K., Chowdhury, T., and Rahman, M.: The
637 earlywood, latewood and xylem vessel chronologies of Teak tree (*Tectona grandis*) provide
638 important insight into xylem hydraulic adjustment to past climate variability, *Agric. For.*
639 *Meteorol.*, 375, 110863, [https://doi.org/https://doi.org/10.1016/j.agrformet.2025.110863](https://doi.org/10.1016/j.agrformet.2025.110863),
640 2025.
- 641 Jihan, M. A. T., Popy, S., Kayes, S., Rasul, G., Maowa, A. S., and Rahman, M. M.: Climate
642 change scenario in Bangladesh: historical data analysis and future projection based on CMIP6
643 model, *Sci. Rep.*, 15, 7856, <https://doi.org/10.1038/s41598-024-81250-z>, 2025.
- 644 Khan, M. S., Rahman, M. M., and Ali, M. A. (eds.): *Red Data Book of vascular plants of*
645 *Bangladesh*. Bangladesh National Herbarium., 179 pp., 2001.
- 646 McDowell, N. G., Sapes, G., Pivovaroff, A., Adams, H. D., Allen, C. D., Anderegg, W. R. L.,
647 Arend, M., Breshears, D. D., Brodribb, T., Choat, B., Cochard, H., De Cáceres, M., De
648 Kauwe, M. G., Grossiord, C., Hammond, W. M., Hartmann, H., Hoch, G., Kahmen, A.,
649 Klein, T., Mackay, D. S., Mantova, M., Martínez-Vilalta, J., Medlyn, B. E., Mencuccini, M.,
650 Nardini, A., Oliveira, R. S., Sala, A., Tissue, D. T., Torres-Ruiz, J. M., Trowbridge, A. M.,
651 Trugman, A. T., Wiley, E., and Xu, C.: Mechanisms of woody-plant mortality under rising
652 drought, CO₂ and vapour pressure deficit, *Nat. Rev. Earth Environ.*, 3, 294–308,
653 <https://doi.org/10.1038/s43017-022-00272-1>, 2022.
- 654 Meinzer, F. C., James, S. A., Goldstein, G., and Woodruff, D.: Whole-tree water transport
655 scales with sapwood capacitance in tropical forest canopy trees, *Plant. Cell Environ.*, 26,



- 656 1147–1155, [https://doi.org/https://doi.org/10.1046/j.1365-3040.2003.01039.x](https://doi.org/10.1046/j.1365-3040.2003.01039.x), 2003.
- 657 Olson, M. E., Anfodillo, T., Gleason, S. M., and McCulloh, K. A.: Tip-to-base xylem conduit
- 658 widening as an adaptation: causes, consequences, and empirical priorities, *New Phytol.*, 229,
- 659 1877–1893, [https://doi.org/https://doi.org/10.1111/nph.16961](https://doi.org/10.1111/nph.16961), 2021.
- 660 Pfautsch, S., Harbusch, M., Wesolowski, A., Smith, R., Macfarlane, C., Tjoelker, M. G.,
- 661 Reich, P. B., and Adams, M. A.: Climate determines vascular traits in the ecologically
- 662 diverse genus *Eucalyptus*, *Ecol. Lett.*, 19, 240–248,
- 663 [https://doi.org/https://doi.org/10.1111/ele.12559](https://doi.org/10.1111/ele.12559), 2016.
- 664 Pretzsch, H., Biber, P., Uhl, E., Dahlhausen, J., Rötzer, T., Caldentey, J., Koike, T., van Con,
- 665 T., Chavanne, A., Seifert, T., Toit, B. du, Farnden, C., and Pauleit, S.: Crown size and
- 666 growing space requirement of common tree species in urban centres, parks, and forests,
- 667 *Urban For. Urban Green.*, 14, 466–479,
- 668 [https://doi.org/https://doi.org/10.1016/j.ufug.2015.04.006](https://doi.org/10.1016/j.ufug.2015.04.006), 2015.
- 669 R Development Core Team: R: A language and environment for statistical computing. R
- 670 Foundation for Statistical Computing, Vienna, Austria., <http://www.r-project.org/>, 2025.
- 671 Rahman, M., Islam, M., Islam, R., and Sobuji, N. A.: Towards Sustainability of Tropical
- 672 Forests: Implications for Enhanced Carbon Stock and Climate Change Mitigation, *J. For.*
- 673 *Environ. Sci.*, 33, 1–000, 2017.
- 674 Rahman, M., Islam, M., and Bräuning, A.: Species-specific growth resilience to drought in a
- 675 mixed semi-deciduous tropical moist forest in South Asia, *For. Ecol. Manage.*, 433, 487–496,
- 676 [https://doi.org/https://doi.org/10.1016/j.foreco.2018.11.034](https://doi.org/10.1016/j.foreco.2018.11.034), 2019.
- 677 Rahman, M., Islam, M., Gebrekirstos, A., and Bräuning, A.: Disentangling the effects of
- 678 atmospheric CO₂ and climate on intrinsic water-use efficiency in South Asian tropical moist
- 679 forest trees, *Tree Physiol.*, 40, 904–916, <https://doi.org/10.1093/treephys/tpaa043>, 2020.
- 680 Rahman, M., Billah, M., Rahman, M. O., Datta, D., Ahsanuzzaman, M., and Islam, M.:
- 681 Disentangling the role of competition, light interception, and functional traits in tree growth
- 682 rate variation in South Asian tropical moist forests, *For. Ecol. Manage.*, 483, 118908,
- 683 [https://doi.org/https://doi.org/10.1016/j.foreco.2020.118908](https://doi.org/10.1016/j.foreco.2020.118908), 2021.
- 684 Schönauer, M., Hietz, P., Schuldt, B., and Rewald, B.: Root and branch hydraulic functioning
- 685 and trait coordination across organs in drought-deciduous and evergreen tree species of a
- 686 subtropical highland forest, *Front. Plant Sci.*, Volume 14, 2023.
- 687 Schuldt, B., Knutzen, F., Delzon, S., Jansen, S., Müller-Haubold, H., Burlett, R., et al.: How
- 688 adaptable is the hydraulic system of European beech in the face of climate change-related
- 689 precipitation reduction?, *N. Phytol.*, 210, 443–458, <https://doi.org/10.1111/nph.13798>, 2016.



- 690 Sperry, J. S., Meinzer, F. C., and McCulloh, K. A.: Safety and efficiency conflicts in
691 hydraulic architecture: Scaling from tissues to trees, *Plant, Cell Environ.*, 31, 632–645,
692 <https://doi.org/10.1111/j.1365-3040.2007.01765.x>, 2008.
- 693 Staal, A., Fetzer, I., Wang-Erlandsson, L., Bosmans, J. H. C., Dekker, S. C., van Nes, E. H.,
694 Rockström, J., and Tuinenburg, O. A.: Hysteresis of tropical forests in the 21st century, *Nat.*
695 *Commun.*, 11, 4978, <https://doi.org/10.1038/s41467-020-18728-7>, 2020.
- 696 Trifilo, P., Raimondo, F., Lo Gullo, M. A., Barbera, P. M., Salleo, S., and Nardini, A.: Relax
697 and refill: xylem rehydration prior to hydraulic measurements favours embolism repair in
698 stems and generates artificially low PLC values, *Plant. Cell Environ.*, 37, 2491–2499,
699 <https://doi.org/https://doi.org/10.1111/pce.12313>, 2014.
- 700 Tyree, M. T. and Zimmermann, M. H.: *Xylem structure and the ascent of sap.*, 2nd ed.,
701 Springer, Berlin, Heidelberg, PP 284, 283 pp., 2002.
- 702 Venturas, M.D., Sperry, J.S., Hacke, U. G.: Plant xylem hydraulics: what we understand,
703 current research, and future challenges., *J. Integr. Plant Biol.*, 59, 356–389,
704 <https://doi.org/https://doi.org/10.1111/jipb.12534>, 2017.
- 705 Viscarra Rossel, R. A., Webster, R., Bui, E. N., and Baldock, J. A.: Baseline map of organic
706 carbon in Australian soil to support national carbon accounting and monitoring under climate
707 change, *Glob. Chang. Biol.*, 20, 2953–2970,
708 <https://doi.org/https://doi.org/10.1111/gcb.12569>, 2014.
- 709 Wright, S. J.: Tropical forests in a changing environment., *Trends Ecol. Evol.*, 20, 553–60,
710 <https://doi.org/10.1016/j.tree.2005.07.009>, 2005.
- 711
- 712
- 713
- 714
- 715
- 716
- 717
- 718
- 719
- 720
- 721
- 722